JOURNAL OF ALGEBRAIC STATISTICS
Volume 13, No. 2, 2022, p. 608 - 620
https://publishoa.com
ISSN: 1309-3452

Structural, Optical and Electrical Properties of Cadmium Sulphide Thin Films Deposited by Spray Pyrolysis Technique

J. Chandrasekar[1, a] and D. Manikandan*[, a]

*[, a] Department of Physics, Arignar Anna Govt. Arts College, Villupuram-605602, Tamilnadu, India, E-mail : a_dmani@yahoo.com
[1]Department of Physics, Tirukkoilur College of Arts and Science, Tirukkoilur-605766, Tamilnadu, India, E-mail : sekarphysics2665@gmail.com

ABSTRACT

At a substrate temperature of 400^o C, spray pyrolysis was used to create thin films of cadmium sulphide with varying molar concentrations. The physical properties of the films were studied as a function of the increase in molar concentration at 0.3, 0.5, 0.7, and 1 M respectively. The films were characterized by different techniques to study their structural, optical, and electrical properties. The X-ray diffraction analysis revealed that the films were polycrystalline in nature. However, when the molar concentration was increased above 1 M, the crystalline quality and the preferential orientation of films deteriorated. Optical measurements showed that the band gap values decreased from 2.6 to 1.8 eV with increasing molar concentrations of 0.3, 0.5, 0.7, and 1 M, respectively. The photoluminescence spectra displayed that all the samples have an emission peak centred at 750 nm. The morphological studies of HR-SEM and HR-TEM from spherical shaped structures and EDX analysis confirm that the metal chalcogenide thin film is metal. The main application of dye-sensitized solar cells with an increase in mole concentration of 0.3, 0.5, 0.7, and 1 M respectively, with an increase in current in short short-circuit density.

1. Introduction

Chalcogens (the column of elements on the periodic table beginning with but not including oxygen) such as sulfur, selenium, and tellurium [**1, 2**].They are extensively studied for applications in catalysis, electronics, thermal insulation, sensors, ceramics, cosmic dust collectors, optical films, and chromatographic molecular separations and for the easy generation of monoliths Chalcogenide gels and aerogels from several binary metal sulfide systems (e.g., GeS_2, ZnS, CdS, TiS_2, NbS_2, La_2S_3, and WSx) have successfully been made solar system [**3-7**]. The film formation takes place from two distinct mechanisms: atom by atom growth or aggregation of colloi'ds formed in solution by an homogeneous reaction. Cadmium sulfide grows according to the first mechanism and films are generally made of microcrystalline grains (size in the range 20 to 80 nm) presenting an hexagonal or cubic structure according to the composition of the solution and the nature of the substrate [**8**]. Metal chalcogenides, now ubiquitously employed in light harvesting and thermoelectrics are taking new strides as active materials for electrochemical devices photocatalysis and chemical sensing [**9-13**]. Key to their further development in these areas has been the introduction of mesoscale porosity into their structure.6 Increased surface area in mesoporous films allows the semiconductor network to interact chemically with exogenous or infiltrating species, thereby revealing new function. Unfortunately, generating ordered mesoporous architectures of metal chalcogenides in films, and preserving them during chemical transformations, has been a challenge that limits systematic delineation of critical architectureproperty relationships in devices [**14-17**] We show here that robust metal chalcogenide architectures can be now constructed fromm colloidal nanocrystal (NC) building units using tailored block copolymer architecture-directing agents (ADAs). By following the thermal process in situ, we show that deliberate engineering of NC-ADA interfacial chemistry was deterministic in maintaining mesoscale ordering through the removal of the ADA to generate hierarchical structures (with control of both nanocrystal and mesopore dimensions). We also demonstrate the robustness of our mesoporous metal chalcogenide architectures by chemically transforming them using cation exchange.

JOURNAL OF ALGEBRAIC STATISTICS
Volume 13, No. 2, 2022, p. 608 - 620
https://publishoa.com
ISSN: 1309-3452

The metal sulphide, selenide and telluride thin samples may be applied as anode in photoelectron chemical devices. The essential necessity of a superior quality of semiconductor photoelectrode for photoelectron chemical devices is large conductivity and large particle dimension. An additional element of photoelectron chemical devices is that the interface of an electrolyte and a semiconducting photoelectrode may produce a superior barrier, consequently make higher photo-voltage yet having inexpensive inferior semiconducting material [**18-26].**

The main aim for solar cell research is to find out ways for safe, high-efficiency solar energy conversion at low cost and to develop reliable and easy to process materials for such devices. One such system is the dye-sensitized solar cell (DSSC), which is regarded as a third generation solar cell, capable of providing facile light-to-electrical energy conversion. Dye-sensitized solar cells (DSSCs) are gaining much attention because of ease of device preparation [**27-29**], relatively low cost production processes, moderate conversion efficiencies and short energy payback time [**30, 31**. DSSC developed by Grâtzel and coworkers in 1991 are a class of cost-effective and environmentally friendly solar cells [**32**]. Such cells are mainly classified as organic dyes and inorganic dyes based devices. Inorganic dyes such as N3, black dye and N719, polypyridine complexes have been widely used as sensitizers in DSSC [**33, 34**]. For many years, ruthenium based complexes were the ‘‘champion’’ dyes for DSSC and some of them were notably distinguished by achieving even 13%efficiency [**35**]. However, despite the fact that high power conversion efficiencies and relatively stable DSSCs have been fabricated using ruthenium sensitizers, the fact remains that even though some ruthenium complexes have shown broad absorption spectra, they generally have modest molar extinction coefficient [**36**],

To elucidate, the crystallographic, morphological, optical characteristics of the samples, X-ray diffractrogram, scanning electron micrograph, absorption properties are studied. In this chapter electrical, and photoelectrochemical properties of the CdS thin films are discussed

2. Experimental

2.1. Material Synthesis

Tin sulphide (CdS) thin films were deposited onto microscopic glass substrates using the spray pyrolysis technique. The precursors of Cadmium chloride $CdCl_2$ and thiourea were dissolved separately in a solution containing deionizer water and isopropyl alcohol in proper ratio. Equal volumes of these two solutions were mixed together and sprayed onto the microscopic glass substrates of 75X25 mm^2 dimensions at the substrate temperature of 350 C. by nebulized spray pyrolysis technique at various molar concentrations (0.3, 0.5, 0.7 and 1 M). The nebulized spray pyrolysis method is very simple technique and low cost to produce CdS thin films. The substrates were first cleaned with a water bath, followed by dipping in con. HCl, acetone and ethanol successively. Finally the substrates were rinsed in deionised water and allowed to dry in a hot air oven. In spray unit, the substrate temperature was maintained with the help of heater, controlled by a feedback circuit. During spray, the substrate temperature was kept constant with an accuracy of 5 K. Spray head and substrate heater kept inside a chamber, provided with an exhaust fan for removing gaseous by-products and vapors from the solvent. The spray head was allowed to move in the X–Y plane using the Micro controller stepper motor, in order to achieve a uniform coating on the substrate. The spray head could scan an area of 200X200 mm with X-movement at a speed of 20 mm/s and Ymovement insteps of 5 mm/s simultaneously. In the spray unit, there was a provision for controlling the spray rate of the solution as well as the presence of carrier gas. The microcontroller device was communicated with PC through the serial port in which the data of each spray could be stored. The values of deposition parameters like solution flow rate, carrier gas pressure and nozzle to substrate distance were kept as 3 ml/min, 1.0 kg/ cm2 and 20 cm, respectively. After deposition, the film was allowed to cool slowly to room temperature and washed with distilled water and then dried

JOURNAL OF ALGEBRAIC STATISTICS
Volume 13, No. 2, 2022, p. 608 - 620
https://publishoa.com
ISSN: 1309-3452

3. Surface morphological studies

3.1. HR-SEM

Scanning electron microscopy (SEM) is a technique for obtaining high-resolution images of surfaces. The nanocomposite material's grain and shape are critical characteristics that influence photocatalytic activity. The HR-SEM images of CdS thin film at a magnification of 1 µm are shown in **Figure 1**a In the HR-SEM the shape of the produced Se-SiO_2 appears to be nano spherical-like micro structure was obtained

3.2. EDS analysis

EDS is a technique for determining the elemental properties of a material. **Figure 1b** depicts the EDS of CdS thin film. It also demonstrates that thin film materials provide techniques for Cd and S.

3.3. HR-TEM

TEM images of the samples results in mean diameters of the CdS of 50 nm respectively. It's possible to obtain in TEM images of the film due to their expectedly 1 M containing a spherical shape structure **its** shows in **Figure 2a**. **Figure 2b and Figure 2c** plot profile and image profile respectively. The finally Figure **2d** show the average particle size was 2.2 nm and the individual particle is shown in **Figure 2a** the images reveal that most of the particles are elongated. However a slight aggregation of particles has been observed in pure samples of thin film. It is observed that, in spite of the agglomeration of nanoparticls, they contain a narrow size distribution.

Figure.1. HR (SEM) study; (a) SEM and (b) EDS analysis by CdS thin film

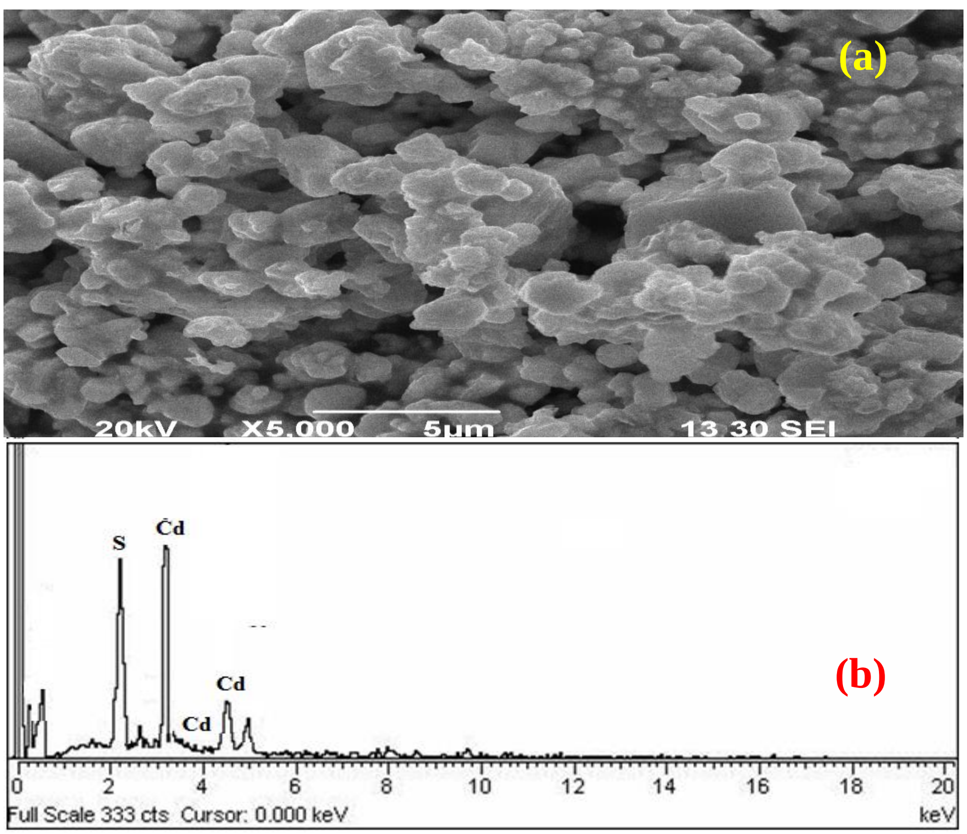

JOURNAL OF ALGEBRAIC STATISTICS
Volume 13, No. 2, 2022, p. 608 - 620
https://publishoa.com
ISSN: 1309-3452

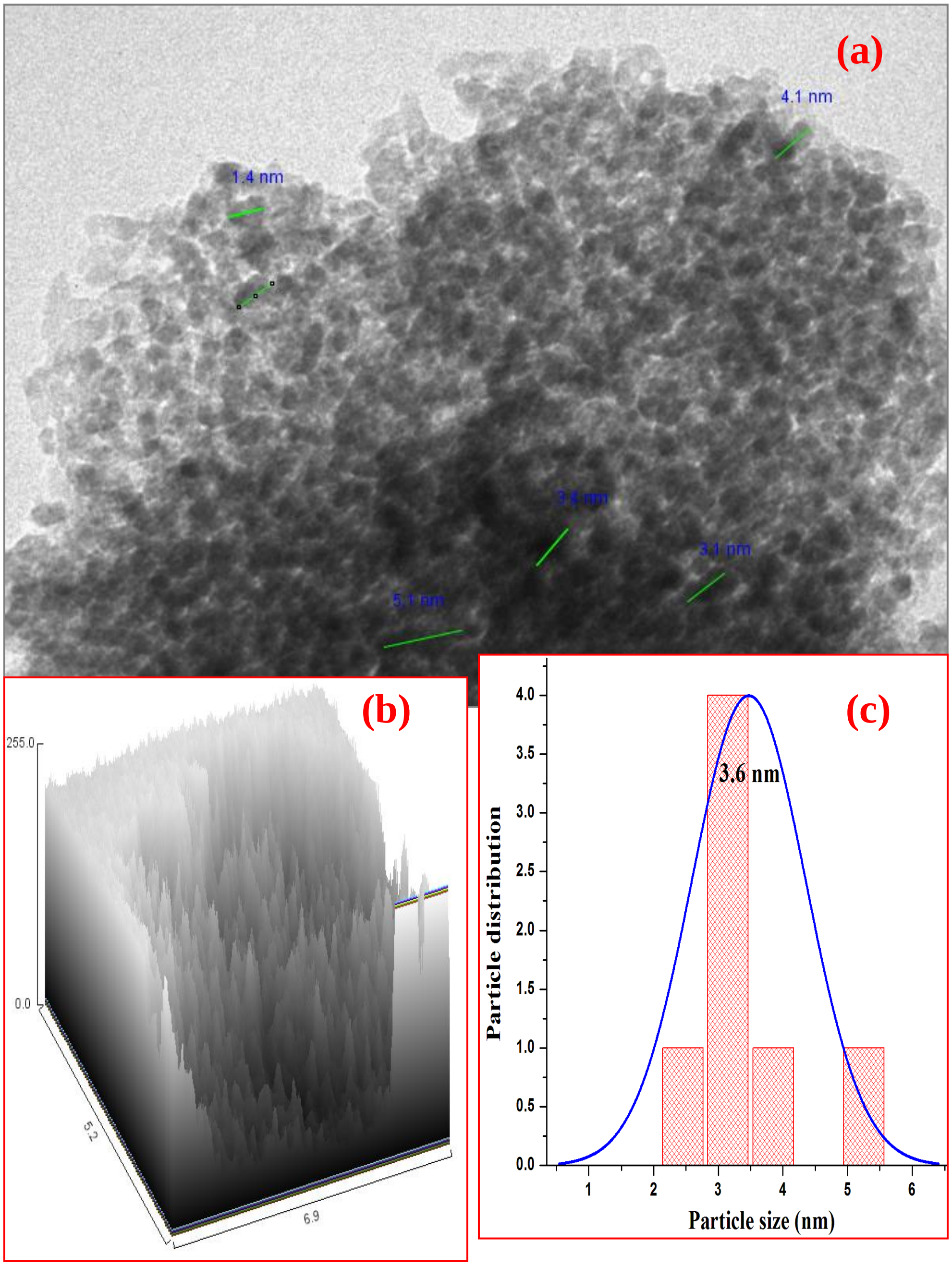

Figure.2. HR (TEM) study of (a) Image CdS thin film, (b) Surface plot and (c) size in a specific area Figure that has been emphasised (a) a really thin film

4. Structural properties

4.1. XRD analysis

Characterization **Figure. 3** shows the XRD pattern of pure CdS thin films. TheXRD results confirm the formation of pure hexagonal phaseof CdS (ICDD card number 06-0314) with (1 0 1) as the pre-ferred orientation. The same plane has been recorded as themain direction of growth in spray pyrolysis deposited CdS by Shaban et al. [**37**] and Rmili et al. [**38**]. This suggests thatincorporation of Cu ions resulted in the enhancement of thedegree of polycrystallinity, i.e. increase of

JOURNAL OF ALGEBRAIC STATISTICS
Volume 13, No. 2, 2022, p. 608 - 620
https://publishoa.com
ISSN: 1309-3452

amorphization ofthe film through suppression of grain growth. The average particle size estimated from X-ray diffractionpattern using the main peak depending on Scherrer's equa-tion: Eq.(1), microstrain (ε) formula, Eq. (2) and dislocation density (δ) formula, Eq. (3) have been employed to calculate the average grain size (D), microstrain (ε) and dislocation density (δ), respectively,

The crystallite size is estimated by Debye Scherrer formula

$$\boldsymbol{D = \frac{K\lambda}{\beta cos\theta}}$$

Where 'β' is the wavelength of CuKα radiation (1.5406 Å), k is shape factor (0.9) is the Bragg's diffraction angle and diffraction line at its full width half maximum intensity (FWHM) in radians, 'λ' is the wavelength of the incident X-ray 'θ' is the angle at which the maximum peak occurs.

The calculated strain (ε) of the pure and doped films using the following equation

$$\varepsilon = \frac{\beta cos\theta}{4}$$

The dislocation density (δ) is estimated from the following relation.

$$\delta = \frac{1}{D^2}$$

The average grain size (DG) has been found in between 24 nm.

where D is the particle size, is the X-ray wavelength(1.5406˚A), ˇ is the full width at half maximum (FWHM) inradian and is the center of the diffraction peak angle value inradian. The FWHM value has been calculated using the X'Pertprogram.The particle size values are obtained using Scherrer's for-mula. The value obtained from Scherrer's equation is smallerthan the real sizes [**39,40**]. Generally the peak broadeningin XRD analysis originates from the instrumental broaden-ing and physical factors such as crystallite size and latticestrain [**41,42**]. In the case of physical factors.

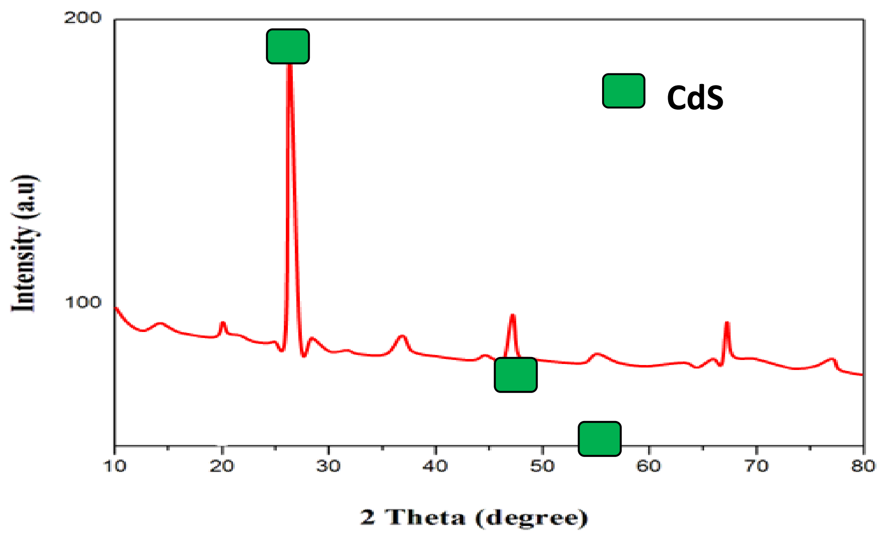

Figure.3. XRD spectra of the CdS (1 M) films

JOURNAL OF ALGEBRAIC STATISTICS
Volume 13, No. 2, 2022, p. 608 - 620
https://publishoa.com
ISSN: 1309-3452

5. Optical studies

5.1. UV-Visible absorption studies

The optical absorption spectra of the film is recorded in wavelength range 350–1100 nm. Hence the optical transmittance (T) with respect to wavelength (λ) of nebulized spray pyrolysed CdS thin film at different molar concentration as shown in **Figure. 4** The optical transmittance spectra indicate a smooth increase and almost saturate at 85% in the visible region. Thin films optical transmittances 65–70% in the 500–800 nm wavelength ranges which is high enough for solar cell applications. Small maxima and minima in the transmittance curves appear due to the multiple interference effect. The multiple interference effect takes place due to high quality films and good surface properties [**43**]. The optical absorption slightly increases and transmittance slightly decreased along with increasing molar concentration 0.3, 0.5, 0.7 and 1 M respectively.

The optical band gap of the CdS thin films decrease in optical band gap with increasing molar concentrations can be due to the increase in the film thickness. The optical band gap values of CdS thin film is decreased from 2.6 to 1.8 eV with increasing molar concentrations 0.3, 0.5, 0.7 and 1 M respectively are shown in **Figure.5.** This value is perfectly matched with previous reported values [**44]**

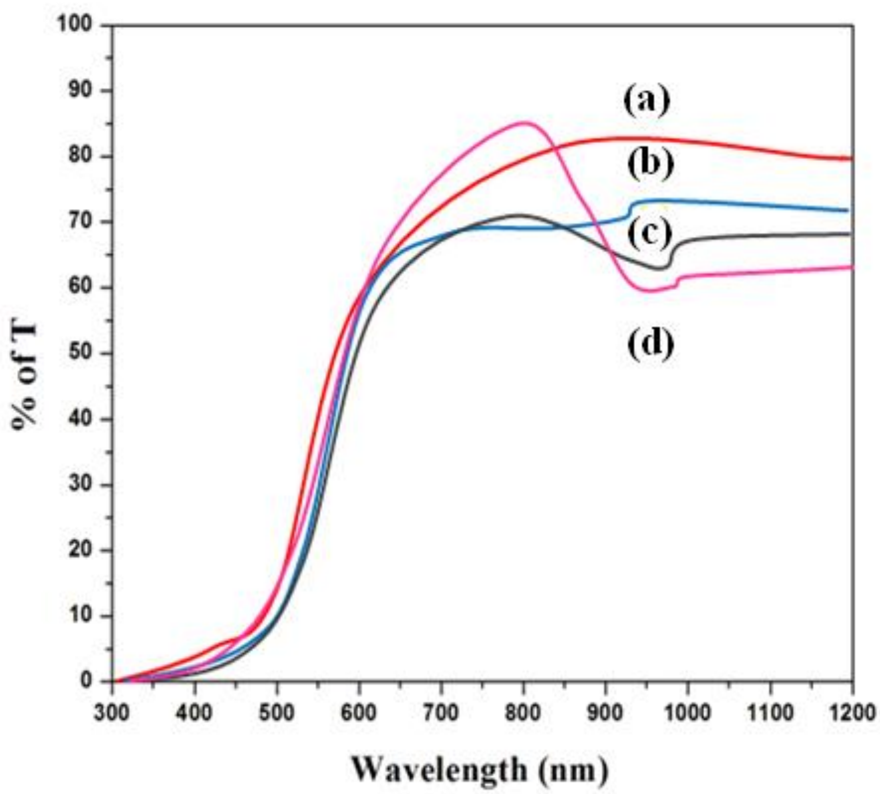

Figure.4. Transmittance of CdS films (a) 0.3 M and (b) 0.5 M, (c) 0.7 M and 1M thin films

JOURNAL OF ALGEBRAIC STATISTICS
Volume 13, No. 2, 2022, p. 608 - 620
https://publishoa.com
ISSN: 1309-3452

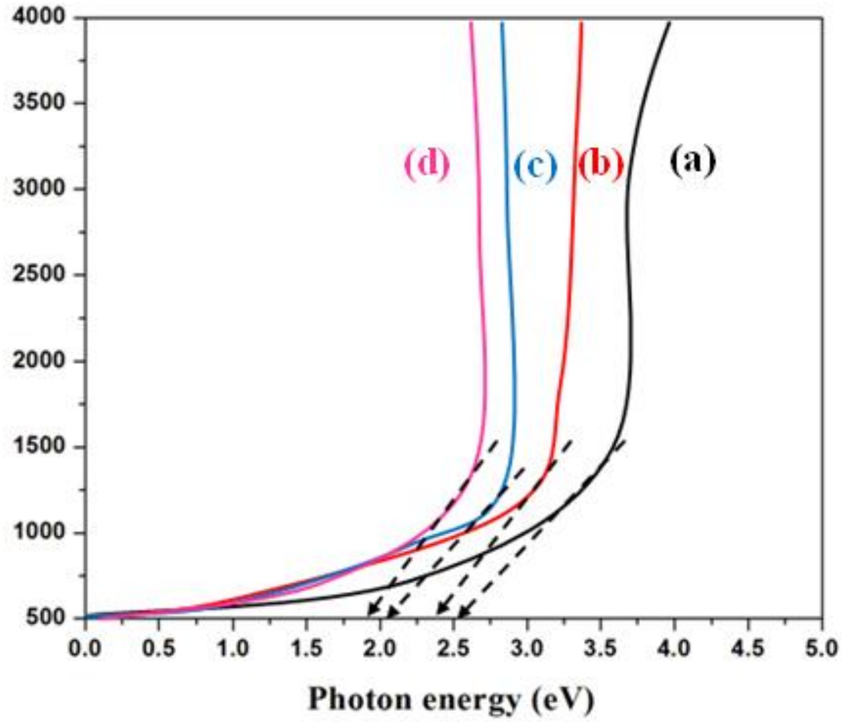

Figure.5 Direct band gap $(\alpha h\nu)^2$ against energy (eV) for CdS thin films (a) 0.3 M and (b) 0.5 M, (c) 0.7 M and 1M thin films

5.2. The extinction coefficient (k)

The extinction coefficient (k) can be obtained from the formula, were evaluated for CdS films by using the relations, where α is the absorption coefficient, λ is the wavelength and k is the extinction coefficient values. The Extinction coefficient (k) can be obtained from the relation,

The extinction coefficient (k) of the films

$$k = \frac{\alpha\lambda}{4\pi}$$

Figures 6 Shows the variation of both k and with wavelength for the layers grown with different molar concentration. The extinction coefficient value of the CdS films is slightly increased in the range from 0.33 to 0.36 with increasing molarities. These values are good agreement with optical properties.

JOURNAL OF ALGEBRAIC STATISTICS
Volume 13, No. 2, 2022, p. 608 - 620
https://publishoa.com
ISSN: 1309-3452

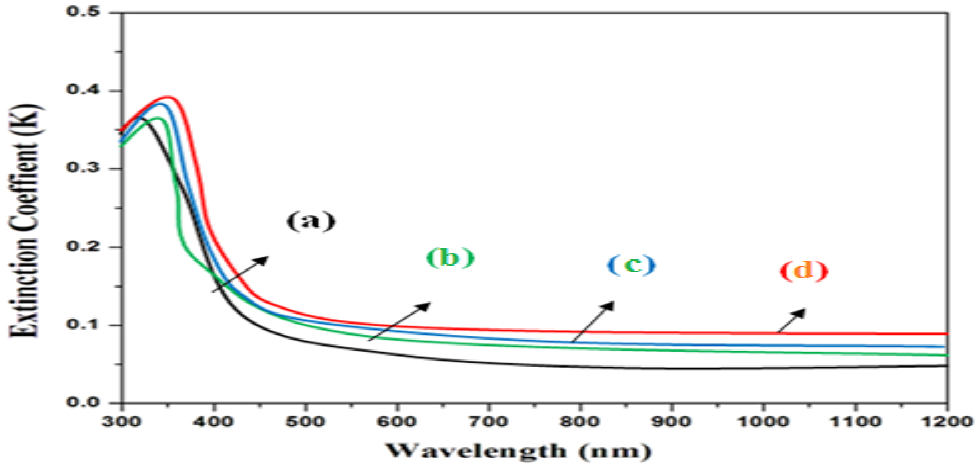

Figure 6. Extinction Coefficient of CdS thin films (a) 0.3 M and (b) 0.5 M, (c) 0.7 M and 1M thin films

5.3. The refractive index

The refractive index is calculated at different wavelength using the relation

$$\mathbf{n} = \frac{1+R^{1/2}}{1-R^{1/2}}$$

In the increase of refractive index with increasing molar concentration of 0.3-1m may be related to increase of the compactness of the films. The high mole concentration of 1 M of CdS, the refractive index is (2.9) in shows in **Figure 7.** The obtained results show that the refractive index is slightly greater than the refractive index of the other mole concentration and then become nearly constant with increasing wavelength. It is attributed to the better crystallinity attributed to the presence of impurities of the prepared film with at increasing mole concentration.

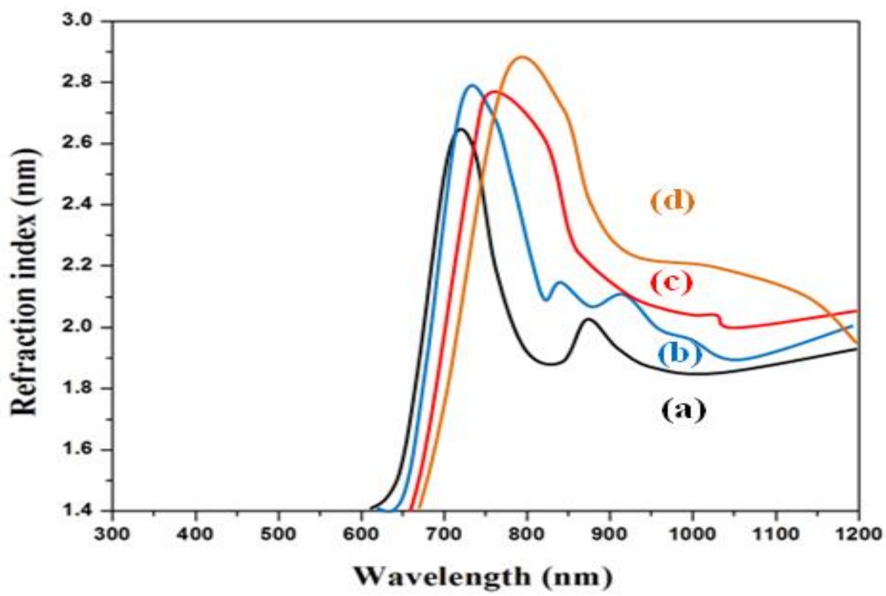

Figure.7. The refractive index (a) 0.3 M and (b) 0.5 M, (c) 0.7 M and 1M CdS thin films

JOURNAL OF ALGEBRAIC STATISTICS
Volume 13, No. 2, 2022, p. 608 - 620
https://publishoa.com
ISSN: 1309-3452

5.4. Photoluminescence spectra

The photoluminescence spectra of CdS thin films with different mole concentration in 0.3-1 M. The spectra of all the samples were recorded in the wavelength range of 500–1000 nm at an excitation wavelength of 500 nm. The figure showed the strong band-edge emission centered at around 730 nm and the intensity of an emission peak was obviously improved when increasing the 1 M concentration in CdS thin films in shown in **Figure.8.** This is because of increase indensity of free excitant and indicated the improvement in crystalline quality of CdS thin film. However, the intensity of band-edge emission was reduced when increasing the 1 M concentration in CdS thin films. The possible reason is the decrease in density of free exciting due to the decline of crystalline quality of CdS thin films. This observation is fairly agrees with the optical measurements [**45, 46**]

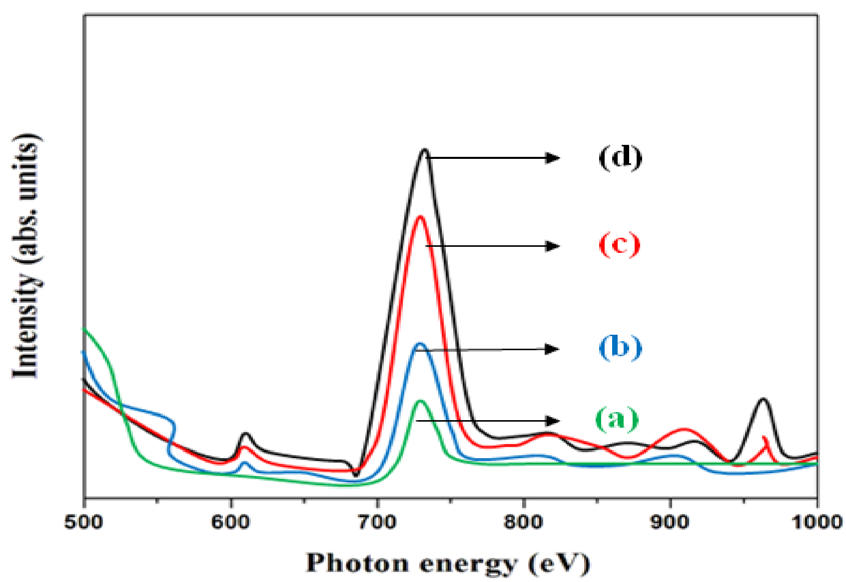

Figure.8. Photoluminescence of (a) 0.3 M and (b) 0.5 M, (c) 0.7 M and 1M CdS thin films

6. Photovoltaic Application

6.1. Synthetic dye based DSSCs

Figure 9 (a-c) the photo current voltage [J–V] properties of dye sensitized solar cells [DSSCs] are depicted in the diagram. The Cadmium sulphide acts as a photo electrode and is deposited on FTO-plate glass at increase of mole concentration 0.3, 0.5, 0.7 and 1 M wirth increase of current in short Short-Circuit Current respectively. Thin films containing synthetic dye (ruthenium dye) are used to make the solar cell (535-bisTBA, N719). The CdS through (1 M) the use of dye as a sensitizer reunites the greatest values of Jsc (Joint Short-Circuit Current Output) (17.0 mA/cm^2 open-circuit voltage Voc (500 mV), fill factor FF (0.94) and productivity g (1.7 percent) [47-53] obtained.

JOURNAL OF ALGEBRAIC STATISTICS
Volume 13, No. 2, 2022, p. 608 - 620
https://publishoa.com
ISSN: 1309-3452

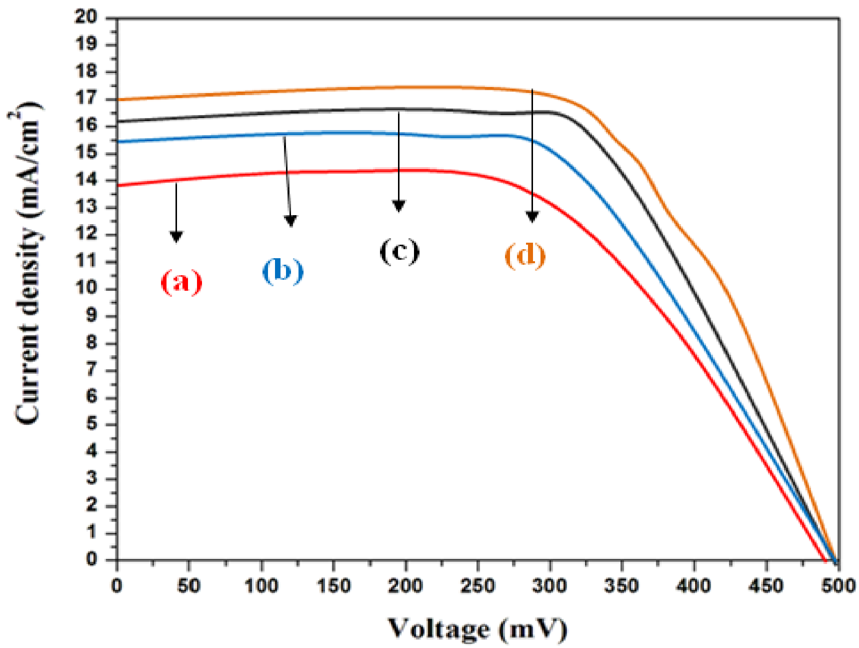

Figure.9. The [J–V] study of CdS thin films (a) 0.3 M and (b) 0.5 M, (c) 0.7 M and 1M CdS thin films

Conclusion

Cadmium sulphide thin films have been prepared by the spray pyrolysis technique**.** A morphological study is present in nanosheet and spherical structures by HR-SEM and HR-TEM. The optical transmittance spectra indicate a smooth increase and almost saturation at 85% in the visible region. CdS thin films decrease in optical band gap with increasing molar concentrations, which can be due to the increase in the film thickness, improving the conversion efficiency of a solar cell application. The main application of CdS thin film is through the use of The use of CdS as a sensitizer (1 M) reunites the highest values of Jsc (Joint Short-Circuit Current Output) (17.0 mA/cm2) with those of low mole concentrations.

Reference

[1] Bag, S.; Trikalitis, P. N.; Chupas, P. J.; Armatas, G. S.; Kanatzidis, M. G. Science 317 (2007) 490–493

[2] Kanatzidis, M. G.; Bag, S. U.S. Patent 7,727,506

[3] Goertz C K, Dusty plasmas in the solar system, *Rev Geophys*, 27(1989)271-292.

[4] Bag, S.; Gaudette, A. F.; Bussell, M. E.; Kanatzidis, M. G. Nat. Chem. 1 (2009) 217–224.

[5] Mohanan, J. L.; Arachchige, I. U.; Brock, S. L. Science, 307 (2005) 397–400.

[6] Brock, S. L.; Arachchige, I. U.; Kalebaila, K. K. Comments Inorg. Chem. 27 (2006) 103–126.

[7] Arachchige, I. U.; Brock, S. L. Acc. Chem. Res. 40 (2007) 801–809.

[8] Lincot. D, R. Ortega-Borges and M. Frornent, Philosophical Magazine B 68 (1994) 185

[9] Reynolds, D.; Leies, G.; Antes, L.; Marburger, R. Phys. Rev. 96 (1954) 533.

[10] Goldsmid, H. J. Thermoelectric Refrigeration; Plenum: New York, 1964.

[11] Lai, C.-H.; Huang, K.-W.; Cheng, J.-H.; Lee, C.-Y.; Hwang, B.-J.; Chen, L.-J. J. Mater. Chem. 20 (2010) 6638.

[12] Kibsgaard, J.; Chen, Z.; Reinecke, B. N.; Jaramillo, T. F. Nat. Mater. 11 (2012) 963.

[13] Xu, J.; Zhang, W.; Yang, Z.; Ding, S.; Zeng, C.; Chen, L.; Wang, Q.; Yang, S. Adv. Funct. Mater. 19 (2009) 1759.

[14] Mohanan, J. L.; Arachchige, I. U.; Brock, S. L. Science, 307 (2005) 397.

[15] Yao, Q.; Brock, S. L. Inorg. Chem, 50 (2011) 9985.

[16] Gacoin, T.; Malier, L.; Boilot, J.-P. Chem. Mater., 9 (1997) 1502.

[17] Fischereder, A.; Martinez-Ricci, M. L.; Wolosiuk, A.; Haas, W.; Hofer, F.; Trimmel, G.; Soler-Illia, G. J. A. A. Chem. Mater, 24 (2012) 1837.

[18] Das D. (1992) Proceedings of Conference of Physics and Technology in Semiconductor Devices and Integrated Circuits.

[19] Yae S., Kobayashi T., Abe M., Nasu N., Fukumuro N., Ogawa S., Yoshida N., Nonamura S., Nakato Y., Matsuda H. Sol. Ener. Mater. Sol. Cells 91 ((2007) 224- 229.

[20] Takabayashi S., Nakamura R., Nakato Y. A nano modified Si/TiO_2 composite electrode for efficient solar water splitting. J. Photochem. Photobio.166 ((2004) 107-113.

[21] Hinogani R., Nakamura Y., Yae S., Nakato Y. Modification of semiconductor surface with ultrafine metal particles for efficient photoelectrochemical reduction of carbon dioxide. Appl. Surf. Sci. 122 ((1997)301- 304.

[22] Hinogani R., Nakamura Y., Yae S., Nakato Y. An approach to ideal

semiconductor electodes for efficient photoelectrochemical reduction of carbon

dioxide by modification with small metal particles. J. Phys. Chem. B 102 (1998) 974-980.

[23] Hankare P., Chate P., Sathe D., Asabe M., Jadhav B. Photoelectrochemical studies of CdSe thin films deposited by dip method. J. Alloys Comp. 474 (2009) 347-350.

[24] RamakrishnaReddy, K.T, N. KoteswaraReddy, andR.W.Miles, "Photovoltaic properties of SnS based solar cells," *Solar Energy Materials and Solar Cells*, vol. 90 (2006) 3041–3046,

[25] Ikuno T, R. Suzuki, K. Kitazumi, N. Takahashi, N. Kato, and K. Higuchi, "SnS thin film solar cells with $Zn1-xMgxO$ buffer layers," *Applied Physics Letters*, vol. 102, no. 19, Article ID193901, 4 pages, 2013.

[26] Sinsermsuksakul. P., K. Hartman, S. B. Kim et al., "Enhancing the efficiency of SnS solar cells via band-offset engineering with a zinc oxysulfide buffer layer," *Applied Physics Letters*, vol. 102, Article ID 053901, 5 pages, 2013.

[27] Maiaugree. W, S. Lowpa, M. Towannang, P. Rutphonsan, A. Tangtrakarn, S. Pimanpang, P. Maiaugree, N. Ratchapolthavisin, W. Sang-Aroon, W. Jarernboon,

V. Amornkitbamrung, A dye sensitized solar cell using natural counter electrode

and natural dye derived from mangosteen peel waste, Sci. Rep. 5 (2015) 15230.

[28] Leyrer. J, R. Hunter, M. Rubilar, B. Pavez, E. Morales, S. Torres, Development of

dye-sensitized solar cells based on naturally extracted dye from the maqui berry (Aristotelia chilensis), Opt. Mater. 60 (2016) 411–417.

[29] Ghann. W, H. Kang, T. Sheikh, S. Yadav, T. Chavez-Gil, F. Nesbitt, J. Uddin,

Fabrication, optimization and characterization of natural dye sensitized solar cell,

Sci. Rep. 7 (2017) 41470.

[30] Song. W., Y. Gong, J. Tian, G. Cao, H. Zhao, C. Sun, Novel photoanode for dyesensitized solar cells with enhanced light-harvesting and electron-collection efficiency, ACS Appl. Mater. Interfaces 8 (2016) 13418–13425.

[31] Wei. L, P. Wang, Y. Yang, R. Fan, Y. Yang, Y. Qiu, Construction of efficient photoanodes for dye sensitized solar cells: TiO2 films with a gradient content of graphene, Sustain Energy Fuels 1 (2017) 1112–1122.

[32] O'regan. B, M. Grfitzeli, A low-cost, high-efficiency solar cell based on dye sensitized, Nature 353 (1991) 737–740.

[33] Wang. Z.S., T. Yamaguchi, H. Sugihara, H. Arakawa, Significant efficiency improvement of the black dye-sensitized solar cell through protonation of TiO2 films,

Langmuir 21 (2005) 4272–4276.

[34] De Angelis F, S. Fantacci, E. Mosconi, M.K. Nazeeruddin, M. Grätzel, Absorption

spectra and excited state energy levels of the N719 dye on TiO2 in dye-sensitized solar cell models, J. Phys. Chem. C 115 (2011) 8825–8831.

[35] Mathew S, A. Yella, P. Gao, R. Humphry-Baker, B.F. Curchod, N. Ashari-Astani, I. Tavernelli, U. Rothlisberger, M.K. Nazeeruddin, M. Grätzel, Dye-sensitized solar cells with 13% efficiency achieved through the molecular engineering of porphyrin sensitizers, Nat. Chem. 6 (2014) 242–247.

[36] Joly. D, L. Pellejà, S. Narbey, F. Oswald, J. Chiron, J.N. Clifford, E. Palomares,

R. Demadrille, A robust organic dye for dye sensitized solar cells based on iodine/

iodide electrolytes combining high efficiency and outstanding stability, Sci. Rep. 4

(2014) 4033.

[37] Shaban M, Mustafa M, El Sayed A. Structural, optical, andphotocatalytic properties of the spray deposited nanoporousCdS thin films; influence of copper doping, annealing, anddeposition parameters. Mater Sci Semicond Process,56 (2016) 329–43.

[38] Rmili A, et al. Structure, optical and electrical properties ofNi-doped CdS thin films prepared by spray pyrolysis. J AlloysCompd, 557 (2013) 53–9.

[39]Medles M, et al. Thin Solid Films 497 (2006) 58–64

[40] Madoun M, et al. Temperature effect on structure andoptoelectronic properties of Bi2S3nanocrystalline thin filmsdeposited by spray pyrolysis method. Mater Sci SemicondProcess 16 (2013) 2084–90.

[41] Mageshari K, Sathyamoorhy R. Mater Sci Semicond Process, 16 (2013) 43–50.

[42] Srinivasan R, Yogamalar R, Chandra A. Mater Res Bull, 45 (2010) 1165–990.

[43] Abdel Rafea. M, N. Roushdy, J. Phys. D 42 (2009) 015–413

[44] Kherchachi. I.B, H. Saidi, A. Attaf, N. Attaf, A. Bouhdjar, Optik 127 (2016) 4043–4046

[**45**]. Santhosh Kumar. K., C. Manoharan, S. Dhanapandian, A. Gowri Manohari, Effect of Sb dopant on the structural, optical and electrical properties of SnS thin films by spray pyrolysis technique, Spectrochimica Acta Part A: Molecular and Biomolecular Spectroscopy 115 (2013) 840–844

[**46**] Moreno-Regino. V.D, F.M. Castañeda-de-la-Hoya, C.G. Torres-Castanedo, J. Márquez-Marín, R. Castanedo-Pérez, G. Torres-Delgado, O. Zelaya-Ángel, Structural, optical, electrical and morphological properties of CdS films deposited by CBD varying the complexing agent concentration, Results in Physics 13 (2019) 102238

[47] RamakrishnaReddy. K.T, N. KoteswaraReddy, andR.W.Miles, "Photovoltaic properties of SnS based solar cells," Solar Energy Materials and Solar Cells, vol. 90 (2006) 3041–3046,

[48] Ikuno. T, R. Suzuki, K. Kitazumi, N. Takahashi, N. Kato, and K. Higuchi, "SnS thin film solar cells with $Zn_{1-x}Mg_xO$ buffer layers," Applied Physics Letters, vol. 102 (2013) 4 Article ID193901,

[49] Sinsermsuksakul. P, K. Hartman, S. B. Kim et al., "Enhancing the efficiency of SnS solar cells via band-offset engineering with a zinc oxysulfide buffer layer," Applied Physics Letters, vol. 102 (2013) 5 Article ID 053901, pages,.

[50] Gopinath G. R. and K. T. Ramakrishna Reddy, Growth of Polycrystalline In2S3 Thin Films by Chemical Bath Deposition Using Acetic Acid as a Complexing Agent for Solar Cell Application, ISRN Condensed Matter Physics, Volume 2013, Article ID 140230, 6 pages http://dx.doi.org/10.1155/2013/140230

[51] Aldakov, D.; Lefrançois, A.; Reiss, P. Ternary and quaternary metal chalcogenide nanocrystals: Synthesis, properties and applications. J. Mater. Chem. C, 1 (**2013**) 3756–3776.

[52] Sandroni, M.; Wegner, K.D.; Aldakov, D.; Reiss, P. Prospects of chalcopyrite-type nanocrystals for energy applications. ACS Energy Lett. 2 (**2017**) 1076–1088.

[53] Wang, H.; Gonzalez-Pedro, V.; Kubo, T.; Fabregat-Santiago, F.; Bisquert, J.; Sanehira, Y.; Nakazaki, J.; Segawa, H. Enhanced carrier transport distance in colloidal PbS quantum dot-based solar cells using ZnO nanowires. J. Phys. Chem. C, 119 (**2015**) 27265–27274.